



3 1176 00169 0156

NASA TM-81604

NASA Technical Memorandum 81604

NASA-TM-81604 19800023979

Performance of Two-Layer Thermal Barrier Systems on Directionally Solidified Ni-Al-Mo and Comparative Effects of Alloy Thermal Expansion on System Life

Stephan Stecura
Lewis Research Center
Cleveland, Ohio

FOR REFERENCE

NOT TO BE TAKEN FROM THIS ROOM

LIBRARY COPY

OCT 24 1980

LANGLEY RESEARCH CENTER
LIBRARY, NASA
HAMPTON, VIRGINIA

October 1980

NASA

PERFORMANCE OF TWO-LAYER THERMAL BARRIER SYSTEMS ON DIRECTIONALLY
SOLIDIFIED Ni-Al-Mo AND COMPARATIVE EFFECTS OF ALLOY
THERMAL EXPANSION ON SYSTEM LIFE

by Stephan Stecura

National Aeronautics and Space Administration

Lewis Research Center

Cleveland, Ohio 44135

SUMMARY

Two-layer thermal barrier coating systems (TBS) for a nickel-aluminum-molybdenum ($\gamma/\gamma' - \alpha$) alloy were evaluated in cyclic furnace tests between 995° and 280° C and between 1095° and 280° C and in natural gas - oxygen torch rig tests between 1250° and 100° C. Two bond coatings and three thermal barrier coating compositions were evaluated. Of the systems tested on $\gamma/\gamma' - \alpha$ substrates, Ni-16.4Cr-5.1Al-0.15Y/ZrO₂-6.1Y₂O₃ showed the most promise. In cyclic furnace tests this system withstood 356 1-hour cycles at 1095° C. This is about 50 percent longer than the performance of a Ni-16.4Cr-5.1Al-0.15Y/ZrO₂-7.8Y₂O₃ system and about 103 percent longer than that of Ni-16.4Cr-5.1Al-0.15Y/ZrO₂-4.0Y₂O₃ system. In a natural gas - oxygen torch rig test at 1250° C the Ni-16.4Cr-5.1Al-0.15Y/ZrO₂-6.1Y₂O₃ on $\gamma/\gamma' - \alpha$ withstood 754 1-hour cycles. This is about 50 percent longer than the performance of a NiCrAl-0.15Y/ZrO₂-7.8Y₂O₃ system and about 63 percent longer than that of a NiCrAl-0.15Y/ZrO₂-4.0Y₂O₃ system. The data also showed that the lives of such systems were decreased by about a factor of 5 at 995° C if the yttrium concentration in the bond coating was increased to 0.35 weight percent from 0.15 weight percent.

N80-32487 #

The coefficient of thermal expansion of the substrate material also has an effect on the life of the TBS. The data indicate that at 1095° C in cyclic furnace tests Ni-16.4Cr-5.1Al-0.15/ZrO₂-7.8Y₂O₃ on $\gamma/\gamma' - \alpha$ substrate had a life of 246 hours, about 50 percent longer than MAR-M200 + Hf and about 134 percent longer than B-1900 + Hf. In the natural gas - oxygen torch rig, at 1250° C, this TBS on $\gamma/\gamma' - \alpha$ had a life of 491 hours, about 60 percent longer than on MAR-M509 and about 30 percent longer than on MAR-M200 + Hf. In this same torch rig at 1250° C, Ni-16.4Cr-5.1Al-0.15/ZrO₂-6.1Y₂O₃ on $\gamma/\gamma' - \alpha$ had a life of 770 hours, about 26 percent longer than on MAR-M509. The data indicate that the compositions of the bond and thermal barrier coating have a more significant effect on TBS life than does the coefficient of thermal expansion of the substrate.

Bond-coating oxidation behavior was found to depend on yttria-stabilized zirconia (YSZ) composition, bond-coating composition, and bond-coating thickness. The bond-coating oxidation rate decreased as the yttria content of the zirconia overlayer increased. The bond-coating oxidation rate increased as the bond-coating yttrium content and thickness increased.

Electron microprobe analysis data showed that yttrium, aluminum, and chromium were not uniformly distributed in the bond coating before testing. The distribution of zirconium in the thermal barrier oxide coating was only slightly nonuniform, but yttrium seemed to be distributed very nonuniformly. During testing, extensive oxidation occurred along the boundaries of the plasma-sprayed bond-coating particles. It is believed that oxygen diffused along these boundaries and that the oxides formed were principally aluminum oxides. It was also found that chromium from the bond coating diffused into $\gamma/\gamma' - \alpha$ and that molybdenum from the substrate diffused into the bond coating.

INTRODUCTION

The search for conventionally cast superalloys capable of withstanding high-temperature stress, oxidation, and hot corrosion for long periods of time has been a continuous effort. The improvement of these alloys has been a pacing factor in the development of aircraft gas turbine engines, since use-temperature limits of superalloys have been increasing at only about 5 to 10 degrees C per year (refs. 1 and 2). Although gamma-prime-strengthened nickel-base superalloys are approaching their upper temperature limits, some improvement can still be made by techniques such as directional solidification (DS) to give better stress-rupture and fatigue lives. Further improvements are possible with eutectic alloy compositions that yield an aligned strengthening phase when directionally solidified (DS eutectics) (ref. 2).

One recent DS eutectic consists of a gamma/gamma-prime matrix composed primarily of nickel (Ni) and aluminum (Al) and fibrous strengthening phase of body-centered-cubic molybdenum (Mo) (α -phase) (refs. 1 to 3). This alloy, $\gamma/\gamma' - \alpha$, has an excellent balance of strength and ductility, but it is not very oxidation resistant at high temperatures. Therefore it must have a protective coating. Existing conventional metallic coatings are not well suited to protect this alloy because its thermal expansion coefficient is significantly lower than those of such coatings. For air-cooled components of this alloy, further protection from environmental attack by use of ceramic thermal barrier coatings is an extremely attractive approach.

Therefore the purpose of this study was to identify two-layer thermal barrier systems, consisting of a thin metallic bond coating and a ceramic thermal barrier coating, that would adhere to $\gamma/\gamma' - \alpha$ for long times at high temperatures. Furthermore, for such a different type of alloy it was also of interest to determine the causes of thermal barrier system failure - the

appearance of a crack in the oxide layer. Thus, the reactions at the substrate - bond coating and bond coating - thermal barrier coating interfaces were studied. Additionally, because of the low expansion of $\gamma/\gamma' - \alpha$, the effect of the thermal expansion coefficient of this substrate as compared with those of conventional superalloys on the life of thermal barrier systems was studied.

EXPERIMENTAL PROCEDURES

Materials

The compositions of the plasma spray powders for the NiCrAlY bond coatings and yttria-stabilized-zirconia ($ZrO_2-Y_2O_3$, referred to as YSZ throughout this report) thermal barrier coatings (both -200 to +325 mesh) are reported in table I. All compositions throughout this report are expressed in weight percent. The alloys used as substrates to study the effect of the substrate coefficient of thermal expansion on the thermal barrier system life in addition to directionally solidified $\gamma/\gamma' - \alpha$ were nickel-base alloys B-1900 + Hf (hafnium) and conventionally and directionally solidified (DS) MAR-M200 + Hf, as well as, the cobalt-base alloy MAR-M509. The compositions of these substrates are also reported in table I. The coefficients of thermal expansion of all these alloys as well as of the bond coating and the YSZ materials at 1100° C are reported in table II (refs. 4-12).

Flat specimens (2.5 cm by 1.2 cm by 0.25 cm) with all corners and edges rounded to about 0.13-centimeter radius were used in the cyclic furnace tests. Flat specimens (7.5 cm by 1.3 cm by 0.5 cm) with corners and edges rounded to about 0.28-centimeter radius were used in the cyclic natural gas-oxygen torch rig tests.

Apparatus and Procedures

Plasma spray coating deposition. - Sample surfaces were grit blast cleaned with high-purity alumina and within 5 minutes the NiCrAlY bond coating was applied with a plasma spray gun (350 A and 28 V). Bond-coating thickness was maintained between approximately 0.008 and 0.017 centimeter. The YSZ thermal barrier coatings were applied with the same plasma spray gun (550 A and 31 V) within 20 minutes after completing application of the bond coating. YSZ thermal barrier coatings were maintained at about a 0.038 ± 0.006 -centimeter thickness on all specimens. Actual coating thicknesses for each $\gamma/\gamma' - \alpha$ specimen are given in tables III and IV, which also contain test results to be described later. Similar bond and thermal barrier coating thicknesses were maintained for specimens used in determining the effect of the substrate coefficient of thermal expansion on the life of the thermal barrier system.

Plasma spraying of both coating layers was done in an open-air environment with argon as the plasma gas and also as the powder feed gas. The plasma-spray-gun-to-specimen distance was maintained at about 13 to 15 centimeters. An attempt was made to maintain the plasma spray gun normal to the surface being sprayed. However, this orientation could not always be maintained when the edges and corners were plasma spray coated.

Cyclic furnace testing. - Coated specimens were heated in air to either 995° or 1095° C. The cycle in both cases consisted in a 6-minute heatup, 60 minutes at temperature, and 60 minutes of cooling to about 280° C. Specimens from the 995° C and 1095° C tests were usually removed from the furnace, where they had cooled to between 350° and 400° C, after every 12 cycles for inspection. Consequently, flat coated specimens that withstood 2000 1-hour cycles to 995° C were cooled to room temperature at least 165

times. Tests were continued until coating failure - the formation of a visible external crack in the YSZ coating. The temperature in the furnace was measured with a platinum/platinum - 13-percent-rhodium thermocouple. The estimated accuracy of the temperature measurements was ± 8 degrees at 1095°C .

Cyclic natural gas - oxygen torch rig testing. - Flat specimens coated with Ni-Cr-Al-Y/ZrO₂-Y₂O₃ thermal barrier systems were tested at about 1250°C in a natural gas - oxygen torch burner rig as shown in figure 1. The hot zone on the coated specimens was about 2.5 centimeters by 1.3 centimeters by 0.6 centimeter (fig. 1). The cycle consisted of a 3-minute heat-up, 60 minutes at 1250°C , and 5 minutes of cooling to about 100°C . The observed surface temperatures were determined with an optical pyrometer. These surface temperatures were corrected to obtain actual surface temperatures by using a calibration curve that was developed from measurements taken on a thermocoupled specimen as discussed in reference 13. Temperature measurements are estimated to be accurate to about ± 25 degrees C at 1250°C .

RESULTS AND DISCUSSION

Cyclic Testing

The furnace data in table III indicate that the performance of the thermal barrier system is very dependent on the yttrium concentration in the NiCrAlY bond coating and the yttria concentration in the YSZ. At 995°C , decreasing the yttrium concentration in the NiCrAlY bond coating from 0.35 to 0.15 significantly improved thermal barrier system life for the same YSZ composition. In this test the Ni-17.0Cr-5.4Al-0.35Y/ZrO₂-7.8Y₂O₃ system failed after 346 to 375 1-hour cycles, but the Ni-16.4Cr-5.1Al-0.15Y/ZrO₂-7.8Y₂O₃ system did not fail even after 2039 1-hour cycles. Furthermore, the data obtained at 1095°C indicated that in

the cyclic furnace test, the $\text{ZrO}_2\text{-6.1Y}_2\text{O}_3$ thermal barrier coating with a Ni-16.4Cr-5.1Al-0.15Y bond coating had a significantly longer life than $\text{ZrO}_2\text{-7.8Y}_2\text{O}_3$ with the same bond coating. These observations are in agreement with the data published in references 13 and 14. The data in table III also show that highly reproducible results (± 5 percent) can be obtained in the cyclic furnace test.

Some of the results of the cyclic furnace test (table III) are confirmed by the natural gas - oxygen torch rig data in table IV. The thermal conditions in the torch rig are more severe than those in the cyclic furnace. In the torch rig a 1250°C surface temperature is reached in 3 minutes, and the specimen cools to about 100°C within 5 minutes after extraction from the flame. Furthermore, since only an area about 2.5 centimeters by 1.3 centimeters by 0.6 centimeter on each side of the specimen was heated, high surface temperature gradients were present. In spite of these more severe thermal conditions, the ranking of the thermal barrier systems in the cyclic furnace and cyclic natural gas - oxygen torch rig tests is identical. The longest life was obtained with the $\text{ZrO}_2\text{-6.1Y}_2\text{O}_3$ thermal barrier coating, followed by that with the $\text{ZrO}_2\text{-7.8Y}_2\text{O}_3$ coating. The system with the $\text{ZrO}_2\text{-4.0Y}_2\text{O}_3$ coating had the shortest lives. For the duplicate specimens tested, coating lives were reproducible to within ± 4 percent.

Thermal barrier system lives in the 1250°C torch rig tests were about twice as long as those in the 1095°C cyclic furnace tests in spite of the higher surface and substrate temperatures, more rapid heating and cooling rates, and more severe temperature gradients. This difference could be due to one or all of the following factors: First, in the torch rig only a small area was heated and this permitted the balance of the specimen to act as a heat sink. Thus the surface could be hotter than the interior. This

provided for a more favorable accommodation of thermal expansion mismatch. Second, in the furnace failures occurred primarily at specimen corners; in the torch rig failures occurred along the edges. Third, there was a more uniform oxide coating thickness on specimens tested in the torch rig. This greater uniformity was obtained by grinding off the buildup (bone shaped) of the YSZ thermal barrier coating present on the ends of the specimens. It was found that the presence of very thick YSZ thermal barrier coating at the ends of the specimens led to rapid failure during testing in the torch rig.

To obtain some understanding of the failure mechanism of the thermal barrier system on $\gamma/\gamma' - \alpha$, specimens were subjected to metallographic and electron microprobe examinations. Also, for the cyclic-furnace-tested specimens, weight gains were measured to determine whether there is a relationship between bond-coating oxidation and thermal barrier system life.

The photomicrograph in figure 2 shows the microstructure of an as-plasma-sprayed thermal barrier system. On the basis of this photomicrograph as well as the photomicrographs from four other locations on this specimen, it was concluded that the plasma-sprayed bond-coating particles were slightly oxidized during coating deposition. This oxidation is indicated by the dark gray stringers between bond-coating particles. There were no major cracks within the bond and thermal barrier coatings. However, microcracks within the plasma-sprayed YSZ thermal barrier coating were encountered, and they are shown in figure 2. This is in agreement with the data reported in reference 15.

Electron microprobe analyses were performed at five different locations on the coated $\gamma/\gamma' - \alpha$ specimens to reveal the distribution of elements within the bond and YSZ coatings and the composition of the oxide stringers formed within the bond coating during coating deposition. Electron micro-

probe continuous-ribbon traverses (30- μ m width analyzed), continuous-line traverses (beam area analyzed), and spectral miniscans (30- μ m widths and beam areas analyzed) were obtained for pertinent elements in the substrate, the bond coating, and the YSZ coating.

Comparing the electron microprobe ribbon traverse in figure 3 with the point-beam traverse of the same area in figure 4 shows that the results of these two procedures convey about the same information. Figures 3 and 4 and traverses from the other four locations indicated that yttrium, aluminum, chromium, and nickel were present throughout the bond coating but that their distributions were not uniform. Areas of high yttrium, aluminum, and even chromium concentration were identified in close proximity to each other. Aluminum peaks such as the one at the bond coating - YSZ coating interface were identified at intervals within the bond coating. No more than four such narrow peaks were encountered across the 0.015-centimeter-thick bond coating, and their locations corresponded with the observed oxide stringers. Thus, the few oxide stringer, such as those shown in the photomicrograph in figure 2, were mostly aluminum oxides with some yttrium oxides and, in a very few cases only, chromium oxides. It is believed that some nickel oxide was also formed. The presence of only a few aluminum oxide stringers points out that the oxidation of the plasma-sprayed bond-coating particles was not too severe. During plasma spraying of the bond coating, it was determined that the thickness of the bond coating increased between 0.002 and 0.003 centimeter per plasma spray pass. Thus there is a rough correlation between the number of spray passes and the number of locations where such oxides were found.

To verify that yttrium was distributed throughout the bond coating, as well as, to verify the distributions of aluminum and chromium in the bond

coating, spectral miniscans for yttrium, aluminum, and chromium were obtained at 5-micrometer intervals. Both 30-micrometer-wide and point-beam areas were analyzed as shown in figures 5(a) and (b), respectively. The data in figure 5 show that there is little or no difference between the results of the two techniques. The data definitely establish that yttrium, aluminum, and chromium were nonuniformly distributed but were also present throughout the bond coating.

The electron microprobe (EMP) ribbon and beam traverses also indicate that, as expected, there was a nearly uniform distribution of zirconium in the thermal barrier oxide coating. Relative drops in concentration indicate regions of pullout or porosity. Fluctuations in yttrium concentration indicate incomplete equilibration during plasma spray powder preparation. No pure yttria particles were detected even with a point beam. However, the presence of fine particles of free yttria cannot be precluded from these data.

Results from X-ray diffraction analyses (ref. 13) showed no free yttria in a 6.2-weight-percent and a 7.9-weight-percent YSZ, which are similar to the materials used in this study. Only cubic and monoclinic zirconia phases were detected, and after testing there was an increase in the amount of cubic phase and a corresponding decrease in the amount of monoclinic phase. It should be remembered that X-ray diffraction analysis is probably not capable of detecting less than 3 weight percent of a minor phase.

Comparing the photomicrographs in figures 2 and 6 indicates that during cyclic furnace testing at 995° and 1095° C the bond coating was significantly oxidized. Less oxidation of the bond coating occurred after 2039 1-hour cycles to 995° C (fig. 6(a)) than after 249 1-hour cycles to 1095° C (fig. 6(b)). At both temperatures, oxidation occurred at the bond coating - ther-

mal barrier interface as well as along the boundaries between plasma-sprayed bond-coating particles and along the bond-coating substrate interface. As shown in figure 6(b)) these were areas where bond-coating particles were totally or nearly totally oxidized. In addition, there were areas where the bond coating was totally oxidized and substrate penetration occurred, as shown in figure 7. In these areas of total bond-coating oxidation, yttrium oxides, aluminum oxides, chromium oxides, and nickel oxides must be present.

At this point, one might be tempted to assign the failure of the thermal barrier coating to these areas of total bond-coating oxidation, as shown, for example, in figure 7. However, these areas were found on the flat surfaces of the tested specimens rather than at the corners and/or the edges of the specimens where the YSZ coatings first failed. Near areas of total bond-coating oxidation no major cracks were observed. Furthermore, it was reported in reference 13 that some thermal barrier systems containing 1.08-weight-percent yttrium bond coatings failed within a short time and after only slight bond-coating oxidation. Additionally, assigning the failure of the thermal barrier coating primarily to the presence of local areas of total bond-coating oxidation does not explain why the 6.1-weight-percent YSZ coating had longer life than the 7.8, 4.0, or 11.5-weight-percent YSZ coatings coupled with the same bond coating (tables III and IV and refs. 13 and 14).

Comparison of the EMP traverses in figures 3, 8, and 9 indicates the major changes that the bond coating and the substrate have undergone as a result of testing. Again, the results in figures 8 and 9 are representative of at least four analyses. The traverses in figures 8 and 9 were obtained under almost the same conditions as the traverse in figure 3. Also, the point-beam traverses were about the same as the 30-micrometer-wide traverses

shown in figures 8 and 9. As can be seen from these figures, a substantial amount of aluminum oxides formed during the 2039 1-hour cycles (no failure) at 995° C and the 249 1-hour cycles (failure) at 1095° C. It is believed that, during cyclic testing, not only is stoichiometric aluminum oxide (Al_2O_3) formed, but also oxides deficient in oxygen. The kinds of oxides formed within the bond coating would affect not only the diffusion of oxygen, but also the increase in the volume of the bond coating. Both these factors might have a significant effect on the life of the thermal barrier system. The positions of the aluminum peaks shown in figures 8 and 9 correspond with the oxide stringers formed within the bond coating. Thus the oxide stringers are primarily aluminum oxides. It may further be concluded that the diffusion of oxygen within the bond coating occurred rapidly along the boundaries of the plasma-sprayed particles.

Comparison of the results in figures 3, 8, and 9 also shows that chromium diffused into the substrate and that molybdenum diffused into the bond coating. Interdiffusion between the bond coating and substrate was greater after 249 1-hour cycles at 1095° C than after 2039 1-hour cycles at 995° C (figs. 8 and 9). Because of the rapid rate of chromium diffusion into the substrate at 1095° C, chromium concentration across the entire bond coating decreased. It is shown in reference 15 that the life of the thermal barrier system is affected by the chromium concentration in the bond coating. The data in this reference show that increasing the chromium concentration in the bond coating from about 16 weight percent to 25 weight percent improved the performance of NiCrAlY/YSZ thermal barrier systems. Thus the decrease of bond-coating chromium concentration by diffusion into the substrate might have had an adverse effect on the life of the thermal barrier system. The data in figures 8 and 9 (particularly in fig. 9) show very extensive diffu-

sion of molybdenum into the bond coating and the near-surface disappearance of molybdenum-rich alpha-strengthening fibers. Such diffusion of molybdenum into the bond coating could have a very detrimental effect on the life of the thermal barrier system. This view was confirmed by an experiment where a Ni-34.0Mo-5.9Al-0.14Y bond coating and a $\text{ZrO}_2\text{-6.1Y}_2\text{O}_3$ thermal barrier coating were plasma sprayed onto a $\gamma/\gamma' - \alpha$ substrate. Results from cyclic furnace tests showed that such a system failed in less than ten 1-hour cycles at 1095°C .

The lives of thermal barrier systems are very sensitive to the bond-coating yttrium concentration (refs. 14 and 15). As mentioned previously the data in figures 3 to 5 show that yttrium was present throughout the as-deposited bond coating. From the electron beam microprobe analyses of the specimen tested for 2039 1-hour cycles at 995°C and of the specimen tested for 249 1-hour cycles at 1095°C , it appears that yttrium was depleted from the inner two-thirds (fig. 8) to the inner three-quarters (fig. 9) of the bond coating, respectively. It also appears that yttrium was concentrated in the outer part of the bond coating. To confirm the higher yttrium concentrations detected near the thermal barrier oxide interface by ribbon electron microprobe scans, spectral miniscans were obtained. As shown previously (fig. 5), 30-micrometer-wide ribbon and point-beam spectral miniscans produced the same results with only the intensities of the peaks varying between the two types of analyses. Thus the ribbon spectral miniscans in figure 10 confirm the yttrium distribution results in figures 8 and 9.

Bond-Coating Oxidation - Weight Gain

In considering the failure mechanism of the thermal barrier system, it is of interest to determine if there was any relationship between the specimen weight gain and thermal barrier system life. The data in figures 11 and

12 show that at both 995° and 1095° C for the Ni-16.4Cr-5.1Al-0.15Y bond coating on Ni-26.4Mo-8.1Al ($\gamma/\gamma' - \alpha$) substrate, weight gains increased as the concentration of yttria in zirconia decreased. This conclusion is valid provided that the bond-coating thickness remains constant, as was the case for the results reported in figures 11 and 12. It was found that the specific weight gain curves for duplicate specimens varied by less than ± 3 percent at 995° C and ± 5 percent at 1095° C.

The Ni-16.4Cr-5.1Al-0.15Y bond coating between the $\gamma/\gamma' - \alpha$ substrate and 7.8-weight-percent YSZ had the lowest rate of oxidation (figs. 11 and 12), and this same bond coating with 6.1-weight-percent YSZ was the most durable in the furnace and torch tests (tables III and IV). This result suggests that bond-coating oxidation is not the only factor governing performance of the thermal barrier system. The 6.1-weight-percent YSZ composition was superior to 4.0- and 7.8-weight-percent YSZ in these specific tests because the ratio of the various phases in YSZ strongly affected the ability of the coating to withstand the imposed cyclic thermal stress.

Bond-coating oxidation is also a function of bond-coating thickness, as shown by the data in figure 13. The data in figure 13(a) for the specimen tested at 995° C show that increasing the thickness of the bond coating caused both the initial rate of weight gain and the ultimate weight gain to increase. This was also the case at 1095° C. However, in the 1095° C test the thermal barrier system with the thinner bond coating failed more rapidly than the one with a thicker bond coating. Measurements of the bond-coating surface roughness indicated a slight decrease in surface roughness with increasing bond-coating thickness. Comparing the data in figure 13(a) with those in figure 13(b) shows that the rate of weight gain at any selected time (number of cycles) also depended on the concentration of yttrium in the

bond coating. As shown in reference 14, bond-coating yttrium concentration strongly influences thermal barrier system life. As the yttrium concentration in the bond coating increases beyond 0.15 weight percent, the life decreases.

The data presented in this report and in references 14 and 15 suggest that since the bond-coating thickness and the yttrium concentration in the bond coating affect the life, the bond coating should be beyond a minimum thickness, have a high degree of thickness uniformity, and have a relatively low yttrium concentration in order to achieve long life.

Effect of Coefficient of Thermal Expansion on Two-Layer Thermal Barrier System Life

The $\gamma/\gamma' - \alpha$ alloy differs from the conventional nickel-base superalloys B-1900 + Hf, MAR-M200 + Hf, and DS MAR M200 + Hf and from the cobalt-base alloy MAR-M509 in that it has a much lower coefficient of thermal expansion (table II). In table II the mean coefficient of thermal expansion for the $\text{ZrO}_2\text{-}7.8\text{Y}_2\text{O}_3$ thermal barrier at 1100° C was assumed to be about 10.3×10^{-6} per degree C. This value was accepted on the basis that the mean coefficient of thermal expansion for 7.8-weight-percent YSZ would not be significantly different from that recorded for 12-weight-percent YSZ. The mean coefficient of thermal expansion for 12-weight-percent YSZ was reported to be 10.3×10^{-6} per degree C (ref. 12).

If the matching of the coefficient of thermal expansion of the substrate with that of the YSZ thermal barrier coating is important, the longest life for the thermal barrier system on the basis of the coefficient-of-thermal-expansion values reported in table II, should be obtained when $\gamma/\gamma' - \alpha$ is the substrate. For this reason cyclic furnace tests were performed in the furnace and in the natural gas - oxygen torch rig on specimens of the vari-

ous superalloys that were coated with similar thicknesses of the same bond and YSZ thermal barrier coatings. The results of these tests are presented in figures 14 and 15. The data from the cyclic furnace tests at 1095° C (fig. 14) show that the low coefficient of thermal expansion of $\gamma/\gamma' - \alpha$ improved the life of the Ni-16.4Cr-5.1Al-0.15/ZrO₂-7.8Y₂O₃ thermal barrier system by more than 130 percent over that of B-1900 + Hf and by about 50 percent over both the conventionally cast and DS MAR-M200 + Hf alloys. This was true in spite of the fact that a high-coefficient-of-thermal-expansion alloy was used as the bond coating (table II). Additional improvements might be achieved by using a bond coating that is very oxidation resistant and also has a low coefficient of thermal expansion. The data in figure 14 show that there was no significant difference in the life of the thermal barrier system when the substrate was conventionally cast or DS MAR-M200 + Hf. However, there was a significant difference in thermal barrier system life between the B-1900 + Hf and MAR-M200 + Hf substrates. The B-1900 + Hf had only a slightly lower coefficient of thermal expansion than DS MAR-M200 + Hf. The reasons for the thermal barrier system failing more rapidly on B-1900 + Hf than on MAR-M200 + Hf remain to be determined.

The data in figure 15 show that in a cyclic natural gas - oxygen torch rig at 1250° C the thermal barrier system on the cobalt-base alloy failed more rapidly than did the same thermal barrier system on conventionally cast MAR-M200 + Hf and $\gamma/\gamma' - \alpha$ substrates. The alloy MAR-M200 + Hf has the highest coefficient of thermal expansion of all the alloys studied. The data in figure 15 show that the low coefficient of thermal expansion of $\gamma/\gamma' - \alpha$ improved the life of the Ni-16.4Cr-5.1Al-0.15-/ZrO₂-7.8Y₂O₃ thermal barrier system by about 30 percent over the conventionally cast nickel-base MAR-M200 + Hf alloy and by about 60 percent over the cobalt-base

MAR-M509 alloy. The data in figure 15 also show that the low coefficient of thermal expansion of $\gamma/\gamma' - \alpha$ improved the life of the Ni-16.4Cr-5.1Al-0.15/ZrO₂-6.1Y₂O₃ system by about 30 percent over MAR-M200 + Hf. Furthermore, the data in figure 15 show that the life of the thermal barrier system depends more on the composition of the YSZ and the composition of the bond coating (fig. 13) than on the coefficient of thermal expansion of the substrate material. Thus the life of the YSZ coating, for the same substrate and the same bond coating, was improved by about 95 percent on MAR-M509 and by about 60 percent on $\gamma/\gamma' - \alpha$ by decreasing the yttria concentration in the ZrO₂ from 7.8 weight percent to 6.1 weight percent (fig. 15).

CONCLUDING REMARKS

The data reported in this study and in references 14 and 15 show that at any temperature the life of thermal barrier coating system is affected by (1) the composition of the bond coating, (2) the concentration of yttria in the zirconia thermal barrier coating, and (3) the coefficient of thermal expansion of the substrate material.

For NiCrAlY bond coatings the yttrium content is very important. Past research at the Lewis Research Center has shown that, when no yttrium is present in the bond coating, the bond coating is rapidly oxidized and coating system failures occur at the bond coating - substrate interface. The presence of yttrium in the bond coating is responsible for the shift of failure location to within the YSZ thermal barrier coating near the bond-coating interface. Yttrium in the bond coating also increases the life of the thermal barrier system. For example, at 990° C, a Ni-16.4Cr-5.8Al-0.32Y/ZrO₂-7.8Y₂O₃ thermal barrier system has at least 230 percent longer life than does a Ni-16.2Cr-5.5Al/ZrO₂-7.8Y₂O₃ ther-

mal barrier system (ref. 15). The first system did not fail even after 1500 1-hour cycles; the second one failed after only 455 1-hour cycles. The electron microprobe data presented in this report show that most of the yttrium in the bond coating during testing diffused toward the bond coating - thermal barrier coating interface. Some yttrium probably diffused into the substrate since a small driving force for this reaction was present. No physical evidence for such diffusion could be obtained with the electron microprobe when using both ribbon and point beams. However, yttrium was detected in the areas near the bond coating - YSZ interface but none was detected within 50 percent of the bond coating away from the bond coating - substrate interface. This is confirmed by the data in figures 8 to 10 for the specimens furnace tested at 995° and 1095° C. This trend in the yttrium diffusion is also confirmed by the data in reference 14. The data in reference 14 show that increasing that yttrium concentration in the bond coating decreased the thickness of the bond coating that was oxidized before the thermal barrier system failed. The data in reference 14 also show that increasing the bond-coating yttrium concentration from 0.15 weight percent to 1.1 weight percent adversely affected the life of the thermal barrier system. Consequently, it was concluded that yttrium diffuses toward the YSZ coating, retards the diffusion of oxygen along the bond-coating particle boundaries, or enhances the formation of a protective oxide scale at the bond coating - YSZ interface. This increases the life of the thermal barrier system. However, why increasing the bond-coating yttrium content from 0.15 weight percent to 1.1 weight percent adversely affects the life of the thermal barrier system remains to be determined. In reference 14 it was shown that for the same substrate and $\text{ZrO}_2\text{-6.2Y}_2\text{O}_3$ thermal barrier coating, the life of the thermal barrier system was improved by about 95

percent when the bond-coating yttrium concentration was decreased from 1.1 weight percent to 0.15 weight percent.

The life of the thermal barrier system can be further improved by changing the bond-coating chromium content. The data in reference 15 show that for the same substrate and $\text{ZrO}_2\text{-}7.8\text{Y}_2\text{O}_3$ thermal barrier coating but with the composition of the bond coating changed from Ni-16.4Cr-5.8Al-0.32Y to Ni-25.7Cr-5.6Al-0.32Y, life was improved by about 110 percent.

The composition of the YSZ has a very important effect on thermal barrier system life, as shown by the data in figure 15. Thus the life of the thermal barrier system was improved by about 95 percent on MAR-M509 alloy substrates and by about 60 percent on $\gamma/\gamma' - \alpha$ alloy substrates by decreasing the yttria concentration in the YSZ thermal barrier coating from 7.8 weight percent to 6.1 weight percent. This result is also supported by the data in references 14 and 15. The data in these references clearly show that total stabilization of monoclinic zirconia to the cubic phase is very undesirable. Thus it was concluded that the $\text{ZrO}_2\text{-}6\text{Y}_2\text{O}_3$ thermal barrier coating is best because of the ratio of crystallographic phases present in this system.

As was mentioned, the coefficient of thermal expansion of the substrate material does affect the life of the thermal barrier system. However, this effect is not as great as that which results from the compositional changes in the bond and thermal barrier coatings. In natural gas - oxygen torch rig tests at 1250° C, decreasing the coefficient of thermal expansion of the substrate by approximately 40 percent from about 18×10^{-6} per degree C to about 10.9×10^{-6} per degree C increased the lives of the

Ni-16.4Cr-5.1Al-0.15Y/ $\text{ZrO}_2\text{-}7.8\text{Y}_2\text{O}_3$ and

Ni-16.4Cr-5.1Al-0.15Y/ $\text{ZrO}_2\text{-}6.1\text{Y}_2\text{O}_3$ thermal barrier systems by about 60

and 30 percent, respectively. Consequently, the data reported in this study and in references 14 and 15 show that the compositional changes in the bond and thermal barrier coatings play a more important role in the life of the thermal barrier system than does the coefficient of thermal expansion of the substrate material.

SUMMARY OF RESULTS AND CONCLUSIONS

A study was conducted in a cyclic furnace and in a cyclic natural gas - oxygen torch rig to identify a thermal barrier coating system (TBS) for a nickel-aluminum-molybdenum ($\gamma/\gamma' - \alpha$) alloy. Also studied were the oxidation of the bond coating and the effect of the substrate thermal expansion coefficient on the life of the thermal barrier system.

1. Thermal barrier system life on the $\gamma/\gamma' - \alpha$ substrate was improved in cyclic furnace tests at 1095° C by about 45 percent and in a cyclic natural gas - oxygen torch rig by about 60 percent when the yttria concentration in YSZ was decreased from 7.8Y₂O₃ to 6.1Y₂O₃. Very insignificant improvement was also achieved when the bond coating composition was optimized.

2. The life of thermal barrier system increased as the coefficient of thermal expansion of the substrate material decreased. Thermal barrier life on $\gamma/\gamma' - \alpha$ at 1095° C in a cyclic furnace was about 50 percent longer than on MAR-M200 + Hf and 130 percent longer than on B-1900 + Hf for the same TBS.

3. The small compositional changes in the bond and thermal barrier coatings have a greater effect on thermal barrier system life than does the significant decrease (about 40 percent) in the coefficient of thermal expansion of the substrate material.

4. Rates of weight gain attributable to bond-coating oxidation increased with increasing bond-coating thickness and decreased as the yttria concentration in YSZ increased from 4 weight percent to 8 weight percent. Thus there seems to be no simple direct relationship between the rate of weight gain and the life of the thermal barrier coating.

5. Principally aluminum oxides, yttrium oxides, some chromium oxides, and possibly nickel oxides formed at the thermal barrier coating - bond coating interface and along the boundaries of the plasma-sprayed particles during testing. With time, the bond coating became heavily oxidized and oxides also formed at the bond coating - substrate interface.

6. Chromium in the bond coating diffused into the substrate, and molybdenum from the substrate diffused into the bond coating. These processes probably had an adverse effect on the thermal barrier coating life. The magnitude of this effect remains to be evaluated.

REFERENCES

1. M. E. Henry, M. R. Jackson, and J. L. Walter, "Evaluation of Directionally Solidified Eutectic Superalloy for Turbine Blade Applications," SRD-78-198, General Electric Co., Schenectady, NY, April 1978. NASA CR-135151, 1978.
2. M. E. Henry, M. R. Jackson, M. F. X. Gigliotti, and P. B. Nelson, "Evaluation of an Advanced Directionally Solidified $\gamma/\gamma' - \alpha$ Mo Eutectic Alloy," SRD-78-191, General Electric Co., Schenectady, NY, January 1979. NASA CR-159416, 1979.
3. F. H. Harf, "Shear Rupture of a Directionally Solidified Eutectic $\gamma/\gamma' - \alpha$ (Mo) Alloy," NASA TM-79118, 1978.
4. "High Temperature, High Strength Nickel Base Alloys," The International Nickel Co., Inc., New York, 3rd edition, 1977.

5. S. S. Manson, p. 6 "Nonferrous Alloys, NiCo," Aerospace Structural Metals Handbook, Volume 5, Code 4213, revised September 1977, Chief Technical Editor, W. F. Brown, Jr., Belfour Stulen, Inc., Traverse City, Mich., 1977.
6. "Materials Reference Card, Cast Nickel Base Alloys," Pratt & Whitney Aircraft, July 31, 1972.
7. S. S. Manson, p. 4 "Nonferrous Alloys, Aerospace Structural Handbook, Volume 5, code 4211, revised December 1971, Chief Technical Editor, W. F. Brown, Jr., Belfour Stulen, Inc., Traverse City, Mich., 1977.
8. "MAR-M200 + Hf Directionally Solidified Coatings," Technical Bulletin TB-1075, Howmet Turbine Components Corp, White Hall, Mich.
9. "MAR-M Alloy 509, Martin Metals," Martin Marietta, Baltimore, Md.
10. "Thermal Expansion Data Sheets for Selected Last High Temperature Alloys," Climax Molybdenum Co. of Michigan, Ann Arbor, Mich.
11. C. E. Lowell, R. G. Garlick, and B. Henry, "Thermal Expansion in the Nickel-Chromium-Aluminum and Cobalt-Chromium-Aluminum Systems to 1200° C," NASA TM X-3268, 1975.
12. K. E. Wilkes and J. F. Lagedorst, pp. 54-55 "Thermophysical Properties of Plasma Sprayed Coatings," Battelle Columbus Labs., Columbus, Ohio, March 1973. NASA CR-121144, 1973.
13. S. Stecura, "Two-Layer Thermal Barrier Coating for Turbine Airfoils - Furnace and Burner Rig Test Results," NASA TM X-3425, 1976.
14. S. Stecura, "Effects of Compositional Changes on the Performance of a Thermal Barrier Coating System," NASA TM-78976, 1978.
15. S. Stecura, "Effects of Yttrium, Aluminum, and Chromium Concentration in Bond Coatings on the Performance of Zirconia-Yttria Thermal Barriers," NASA TM-79206, 1979.

TABLE I. - COMPOSITIONS OF SPRAY POWDERS AND SUPERALLOY SUBSTRATES

Element	Bond coating, NiCrAlY	Thermal barrier, ZrO ₂ -Y ₂ O ₃	Nickel-base substrates				Cobalt-base substrate, MAR-M509
			Ni-Al-Mo	B-1900 + Hf	MAR-M200 + Hf	DS MAR-M200 + Hf	
			Composition, wt%				
Al	^a 5.1 - 5.4	0.009	8.10	6.17	5.03	5.30	(b)
B	<.001	<.001	.01	<.003	.02	.02	<0.001
C	.007	(b)	.005	.008	.12	.16	.63
Ca	(b)	.058	.001	.001	.001	.001	.001
Co	.035	<.005	.002	10.43	10.19	9.97	Major
Cr	^a 16.4 - 17.0	(b)	.01	8.24	8.61	8.22	23.55
Cu	.014	(b)	.08	<.002	<.10	<.01	<.01
Fe	.041	.041	.03	.06	.35	.21	.58
Hf	<.01	1.60	.05	1.22	1.97	2.25	.01
K	<.001	<.001	2.50	<.001	<.001	<.001	<.001
Li	<.001	<.001	.001	↓		↓	<.001
Mg	<.001	.032	.001	↓	↓	↓	<.001
Mn	.011	<.001	.001	↓	↓	↓	<.01
Mo	<.005	<.005	26.40	5.79	(b)	(b)	.005
Na	<.001	<.001	0.40	<.001	<.001	<.001	<.001
Nb	.038	.005	.005	<.005	1.18	1.05	.005
Ni	Major	.027	Major	Major	Major	Major	10.62
O ₂	.020	(b)	(b)	(b)	(b)	(b)	(b)
P	.01	↓	.01	(b)	↓	↓	(b)
Pb	(b)	↓	.06	<.005	↓	↓	.005
S	.01	↓	.01	<.01	↓	↓	<.01
Si	.082	.057	.01	<.01	.20	<.10	.22
Sr	.01	.01	.001	(b)	(b)	(b)	(b)
Ta	<.05	.02	.13	4.13	(b)	(b)	3.77
Ti	.012	.045	.002	(b)	1.99	2.25	.16
V	.032	<.001	.006	<.001	<.001	<.001	.69
W	.01	<.005	.03	.01	11.65	11.60	6.96
Y	^a 0.15 - 0.35	^c 3.1 - 6.1	.001	(b)	(b)	(b)	(b)
Zn	<.05	<.05	.03	<.05	<.05	<.05	<.05
Zr	(b)	Major	.006	.07	.09	.06	.53

^aAluminum, chromium, and yttrium concentrations in NiCrAlY bond coatings are specified in tables of experimental data.

^bNot determined.

^cYttria concentrations for yttria-stabilized zirconias used are specified in tables of experimental data.

TABLE II. - MEAN COEFFICIENTS OF THERMAL EXPANSION AT 1100° C FOR VARIOUS MATERIALS USED IN STUDY TO DETERMINE EFFECT OF THERMAL EXPANSION ON THERMAL BARRIER SYSTEM LIFE

Materials	Coefficient of thermal expansion, per deg C	Reference	Remarks
$\gamma/\gamma' - \alpha$	10.9×10^{-6}	2	Mean longitudinal expansion
B-1900 + Hf	16.3	4,5,6	Representative coefficient
MAR-M200 + Hf	17.6	4,6,7	Representative coefficient
DS MAR M200 + Hf	16.7	8	-----
MAR-M509	18.2	6,9,10	Representative coefficient
Ni-16.4Cr-5.1Al-0.15Y	19.0	11	Based on Ni-16Cr-6Al coefficient
ZrO ₂ -12Y ₂ O ₃	10.3	12	-----
ZrO ₂ -7.8Y ₂ O ₃	10.3	-----	No data. First approximation based on ZrO ₂ -12Y ₂ O ₃ coefficient

TABLE III. - PERFORMANCE OF VARIOUS THERMAL BARRIER SYSTEMS ON Ni-Al-Mo ($\gamma/\gamma' - \alpha$) SUBSTRATE AS DETERMINED BY CYCLIC FURNACE TESTS^a

Bond coating		Thermal barrier coating		Number of cycles to failure ^b
Composition, wt%	Thickness, cm	Composition, wt%	Thickness, cm	
995° - 280° C				
Ni-17.0Cr-5.4Al-0.35Y ↓	0.010	ZrO ₂ -7.8Y ₂ O ₃	0.038	346
	.010	ZrO ₂ -7.8Y ₂ O ₃	.039	355
	.016	ZrO ₂ -7.8Y ₂ O ₃	.050	375
Ni-16.4Cr-5.1Al-0.15Y ↓	0.014	ZrO ₂ -4.0Y ₂ O ₃	0.004	C1735
	.017	ZrO ₂ -4.0Y ₂ O ₃	.044	C1735
	.011	ZrO ₂ -6.1Y ₂ O ₃	.044	C1756
	.012	ZrO ₂ -6.1Y ₂ O ₃	.038	C1756
	.008	ZrO ₂ -7.8Y ₂ O ₃	.040	C1910
	.010	↓	.039	C1910
	.014		.037	C2039
	.014		.037	C2039
				C2039
1095° - 280° C				
Ni-16.4Cr-5.1Al-0.15Y ↓	0.012	ZrO ₂ -4.0Y ₂ O ₃	0.037	166
	.013	ZrO ₂ -4.0Y ₂ O ₃	.039	182
	.013	ZrO ₂ -6.1Y ₂ O ₃	.039	356
	.014	ZrO ₂ -6.1Y ₂ O ₃	.046	356
	.013	ZrO ₂ -7.8Y ₂ O ₃	.037	242
	.014	ZrO ₂ -7.8Y ₂ O ₃	.041	249

^aSolid specimens were about 2.5 cm by 1.3 cm by 0.25 cm.

^bCycles consisted of a 6-min heatup, 60 min at temperature, and 60 min of cooling to about 280° C. Test stopped whenever a visible crack occurred (failure). Specimens inspected about every 12 cycles.

Each of the cycles-to-failure values represents one specimen.

^cNo failure.

TABLE IV. - PERFORMANCE OF VARIOUS THERMAL BARRIER SYSTEMS ON Ni-Al-Mo (γ/γ' - α) SUBSTRATE AS DETERMINED AT 1250° C BY CYCLIC NATURAL GAS - OXYGEN TORCH RIG TESTS^a
[Bond coating (in wt%), Ni-16.4Cr-5.1Al-0.15Y; bond-coating thickness, 0.013 cm.]

Thermal barrier coating		Number of cycles to failure ^b
Composition, wt%	Thickness, cm	
ZrO ₂ -4.0Y ₂ O ₃	0.041	447
	.052	479
ZrO ₂ -6.1Y ₂ O ₃	0.032	746
	.035	783
ZrO ₂ -7.8Y ₂ O ₃	0.031	478
	.034	515

^aSolid specimens were about 7.6 cm by 1.3 cm by 0.5 cm.

^bCycle consisted of a 3-min heatup, 60 min at 1250° C, and 5 min of cooling to about 100° C. Testing stopped whenever a visible crack occurred (failure). Each of the cycles-to-failure values represents one specimen. Specimens were inspected at least once every 16 cycles.

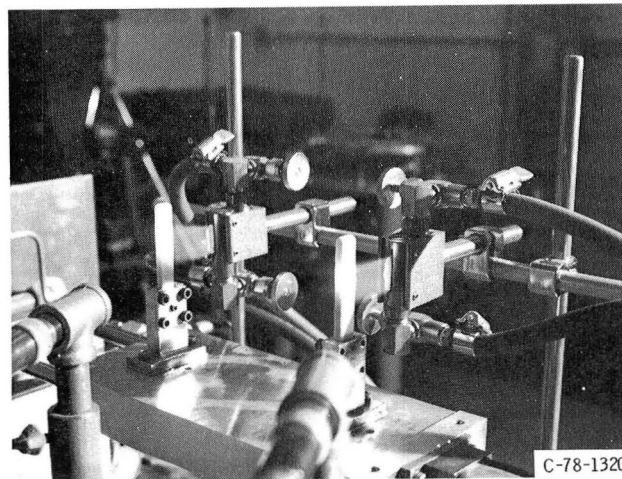


Figure 1. - Natural gas - oxygen torch burner rig and solid specimens coated with NiCrAlY bond coating and ZrO₂-Y₂O₃ thermal barrier coating.

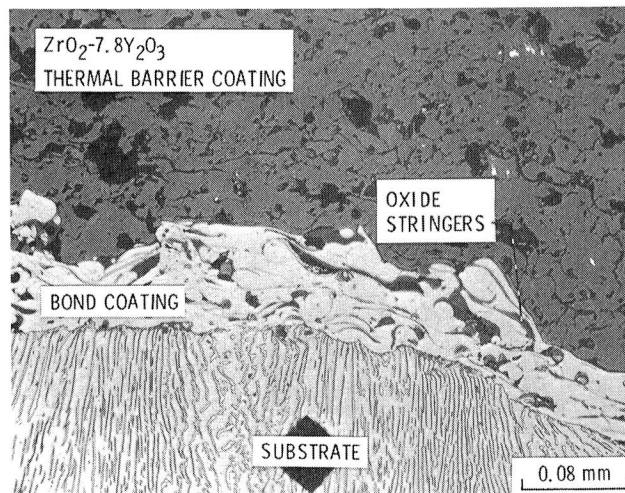


Figure 2. - Optical photomicrograph of edge of a γ/γ' - α coupon as coated with Ni-16.4Cr-5.1Al-0.15Y bond coating and ZrO₂-7.8Y₂O₃ thermal barrier coating.

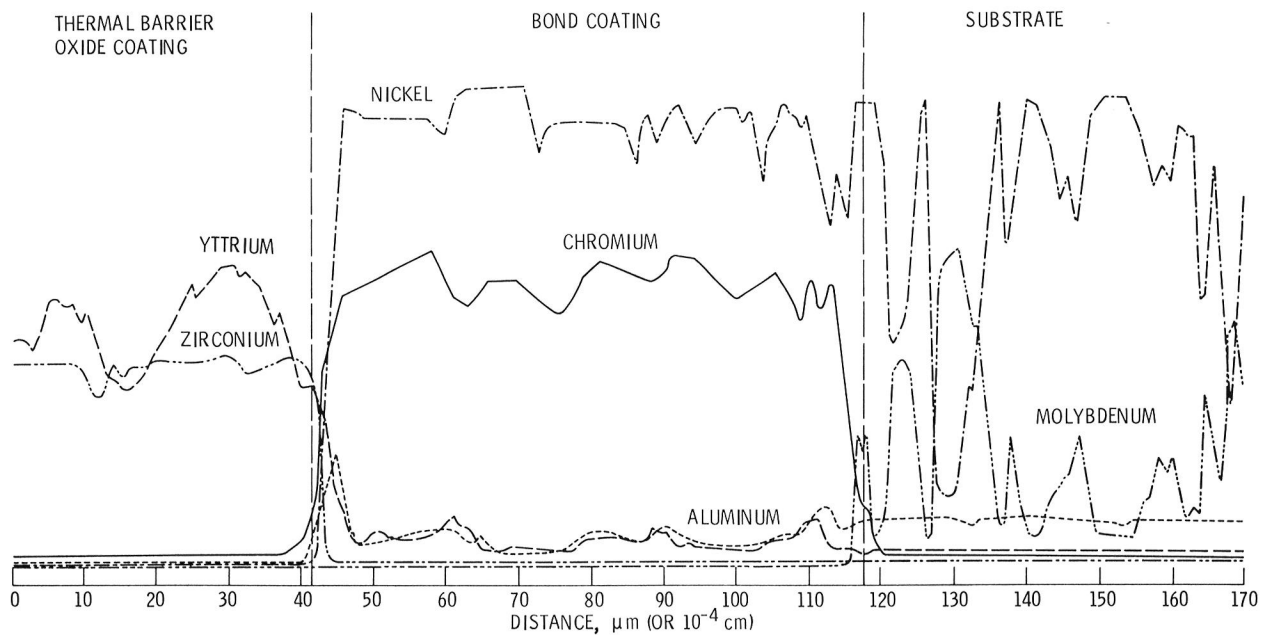


Figure 3. - Electron microprobe continuous-ribbon traverse (30- μm width analyzed) of thermal barrier system consisting of Ni-16.4Cr-5.1Al-0.15Y and ZrO₂-7.8Y₂O₃ as plasma sprayed onto Ni-Al-Mo (γ/γ' - α) alloy substrate.

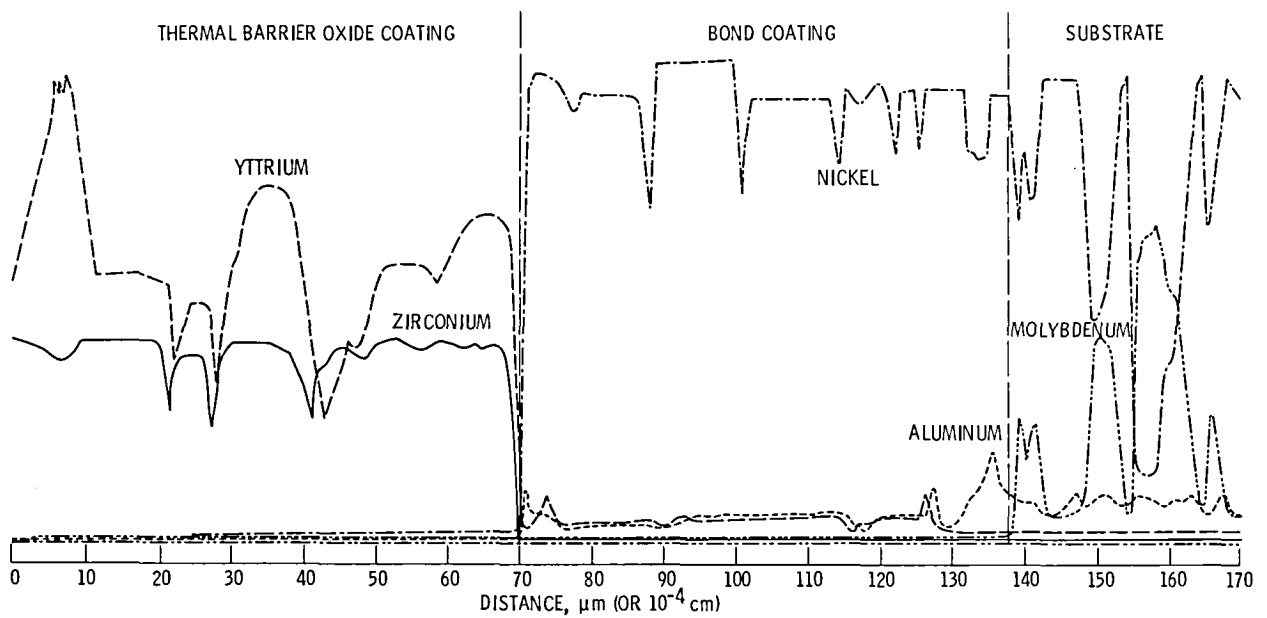


Figure 4. - Electron microprobe of continuous point-beam traverse of thermal barrier system consisting of Ni-16, 4Cr-5, 1Al-0, 15Y and $\text{ZrO}_2\text{-}7.8\text{Y}_2\text{O}_3$ as plasma sprayed onto Ni-Al-Mo (γ/γ' - α) alloy substrate.

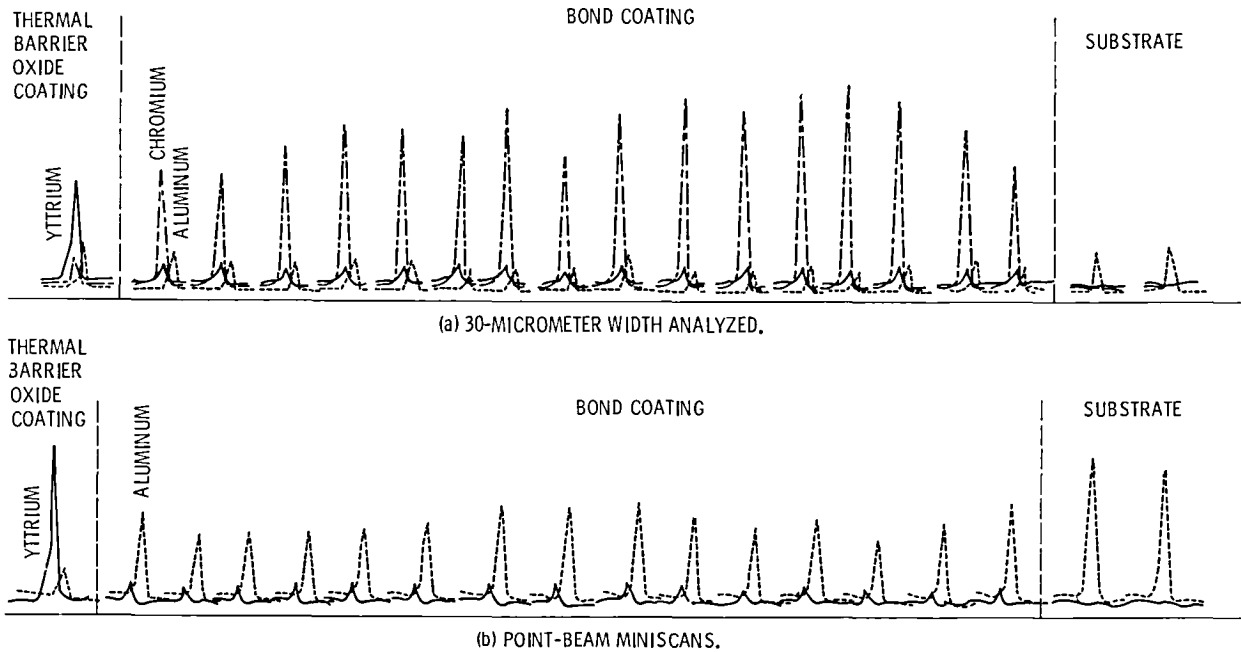
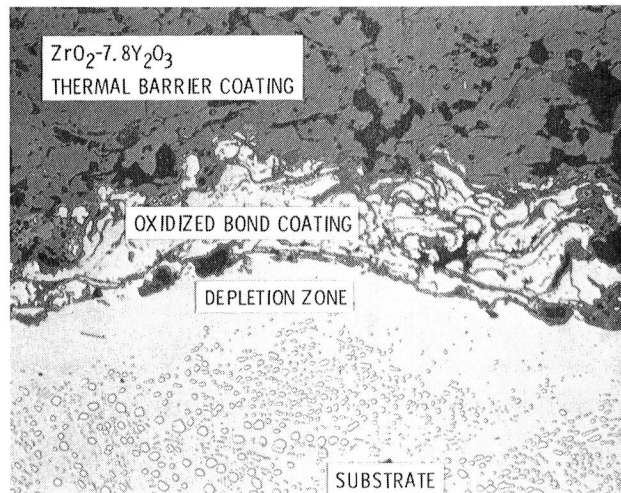
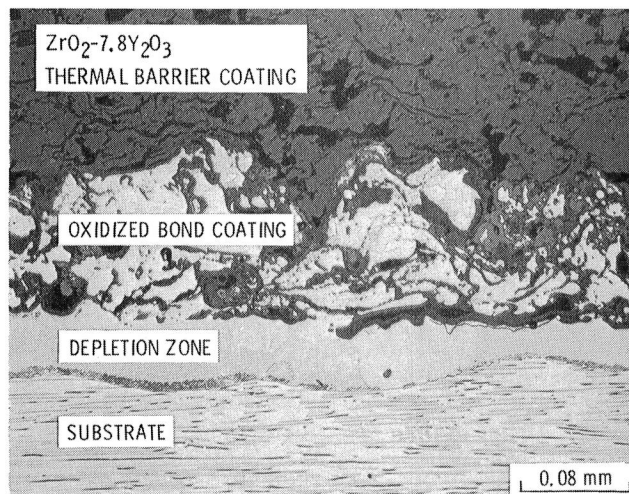


Figure 5. - Spectral miniscans for pertinent peaks of elements in thermal barrier system consisting of Ni-16, 4Cr-5, 1Al-0, 15Y and $\text{ZrO}_2\text{-}7.8\text{Y}_2\text{O}_3$ as plasma sprayed onto Ni-Al-Mo (γ/γ' - α) alloy substrate. Spectral miniscans obtained at about 5- μm intervals.



(a) EDGE AFTER 2039 1-hr CYCLES AT 995⁰ C.



(b) FLAT SURFACE AFTER 249 1-hr CYCLES AT 1095⁰ C.

Figure 6. - Optical photomicrographs of γ/γ' - α coupon specimens coated with Ni-16.4Cr-5.1Al-0.15Y bond coating and $\text{ZrO}_2\text{-7.8Y}_2\text{O}_3$ thermal barrier coating after testing. (Cycle - 6-min heatup, 60 min at temperature, and 60 min of cooling to about 280⁰ C.)

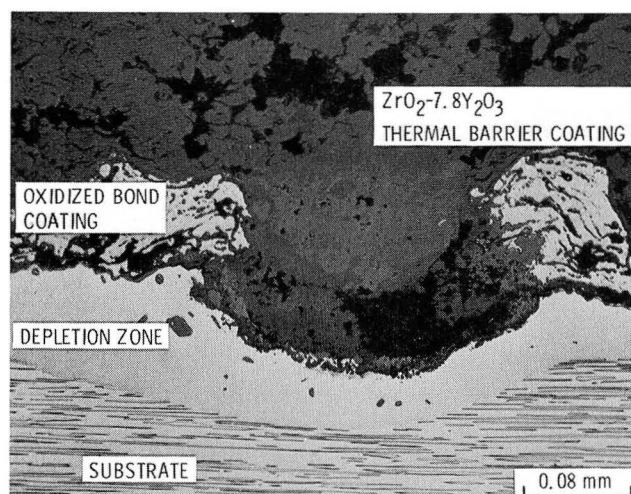


Figure 7. - Optical photomicrograph of a flat surface of a $\gamma/\gamma' - \alpha$ coupon specimen coated with Ni-16, 4Cr-5, 1Al-0.15Y bond coating and $\text{ZrO}_2-7.8\text{Y}_2\text{O}_3$ thermal barrier coating after 249 1-hr cycles at 1095°C . (Cycle - 6-min heatup, 60 min at temperature, and 60 min of cooling to about 280°C .)

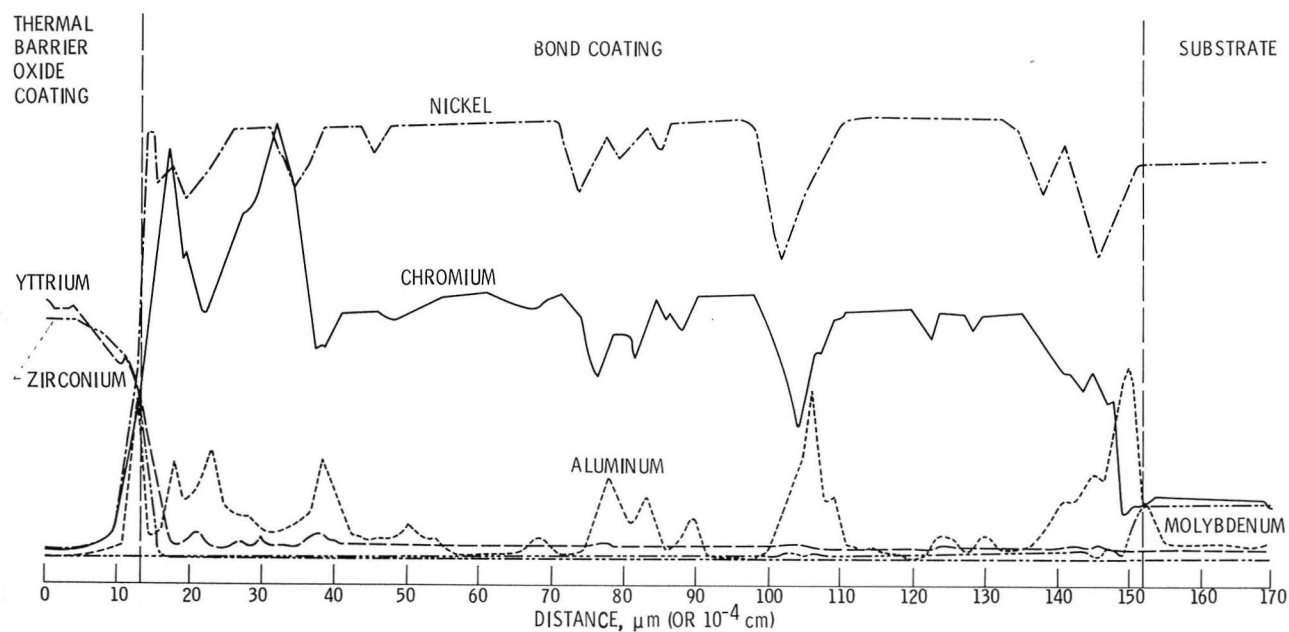


Figure 8. - Electron microprobe continuous-ribbon traverse of thermal barrier system consisting of Ni-16, 4Cr-5, 1Al-0.15Y and $\text{ZrO}_2-7.8\text{Y}_2\text{O}_3$ on Ni-Al-Mo ($\gamma/\gamma' - \alpha$) after 2039 1-hr cycles at 995°C and no failure. (Cycle - 6-min heatup, 60 min at temperature, and 60 min of cooling to about 280°C .)

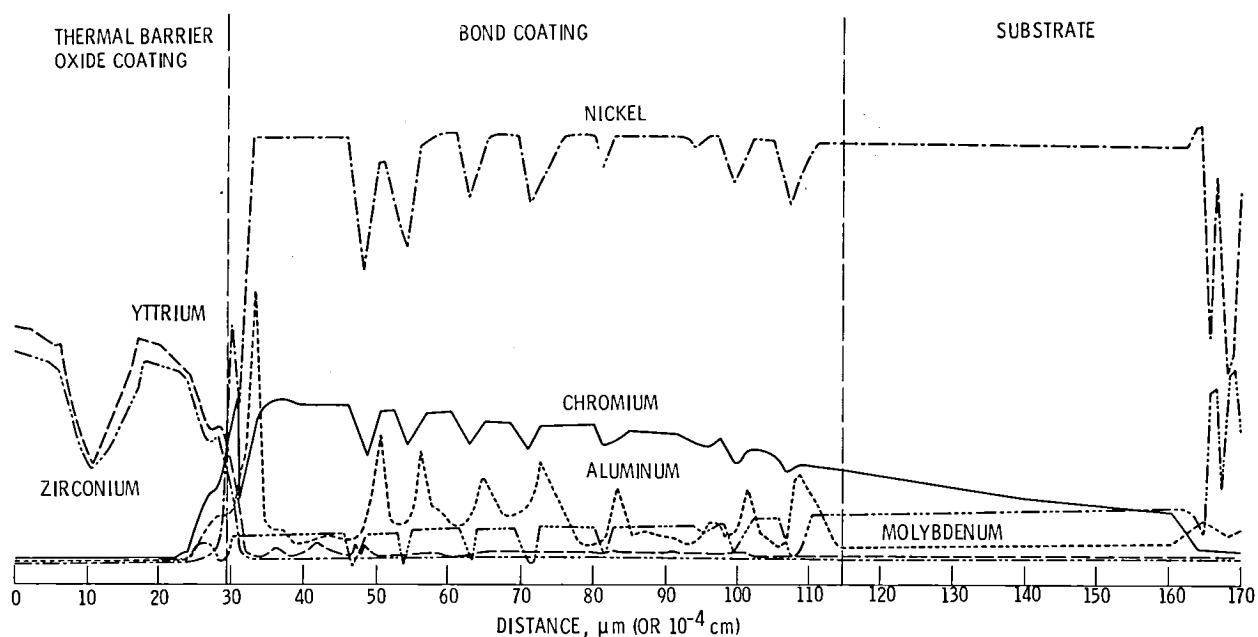


Figure 9. - Electron microprobe continuous-ribbon traverse of thermal barrier system consisting of Ni-16, 4Cr-5, 1Al-0, 15Y and $\text{ZrO}_2\text{-}7.8\text{Y}_2\text{O}_3$ on Ni-Al-Mo ($\gamma/\gamma' - \alpha$) after 249 1-hr cycles at 1095°C and failure. (Cycle - 6-min heatup, 60 min at temperature, and 60 min of cooling to about 280°C .)

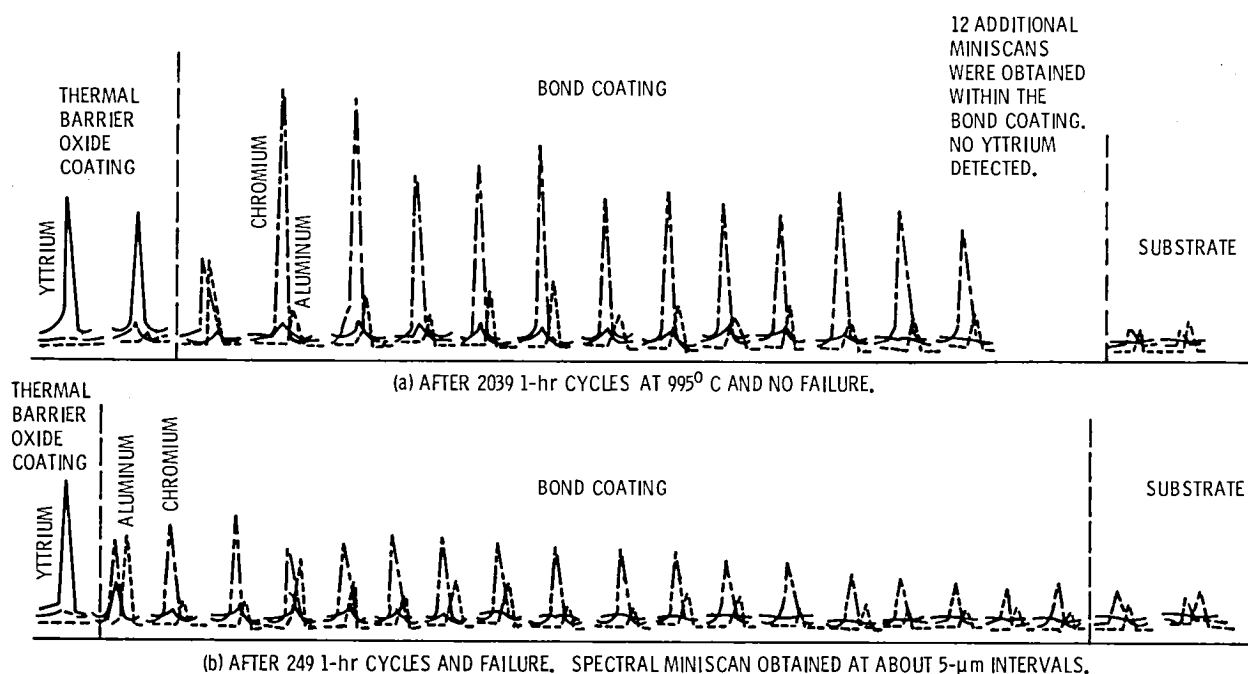


Figure 10. - Spectral miniscans (30- μm width analyzed) for aluminum, chromium, and yttrium in the thermal barrier system consisting of Ni-16, 4Cr-5, 1Al-0, 15Y and $\text{ZrO}_2\text{-}7.8\text{Y}_2\text{O}_3$ on Ni-Al-Mo ($\gamma/\gamma' - \alpha$). (Cycle - 6-min heatup, 60 min at temperature, and 60 min of cooling to about 280°C .)

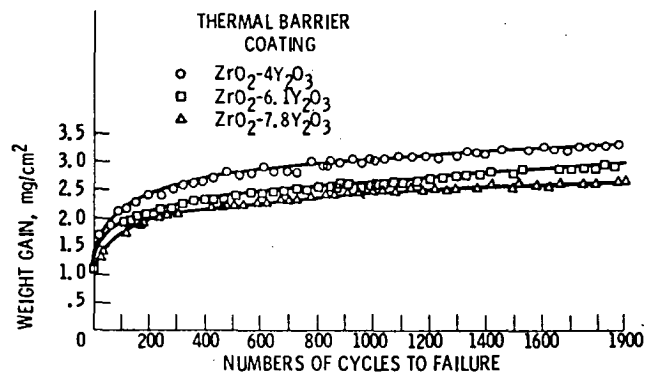


Figure 11. - Effect of yttria concentration in zirconia thermal barrier coating on specimen weight gain at 995°C . (Cycle - 6-min heatup, 60 min at temperature, and 60 min of cooling to about 280°C .) Bond coating, Ni-16.4Cr-5.1Al-0.15Y.

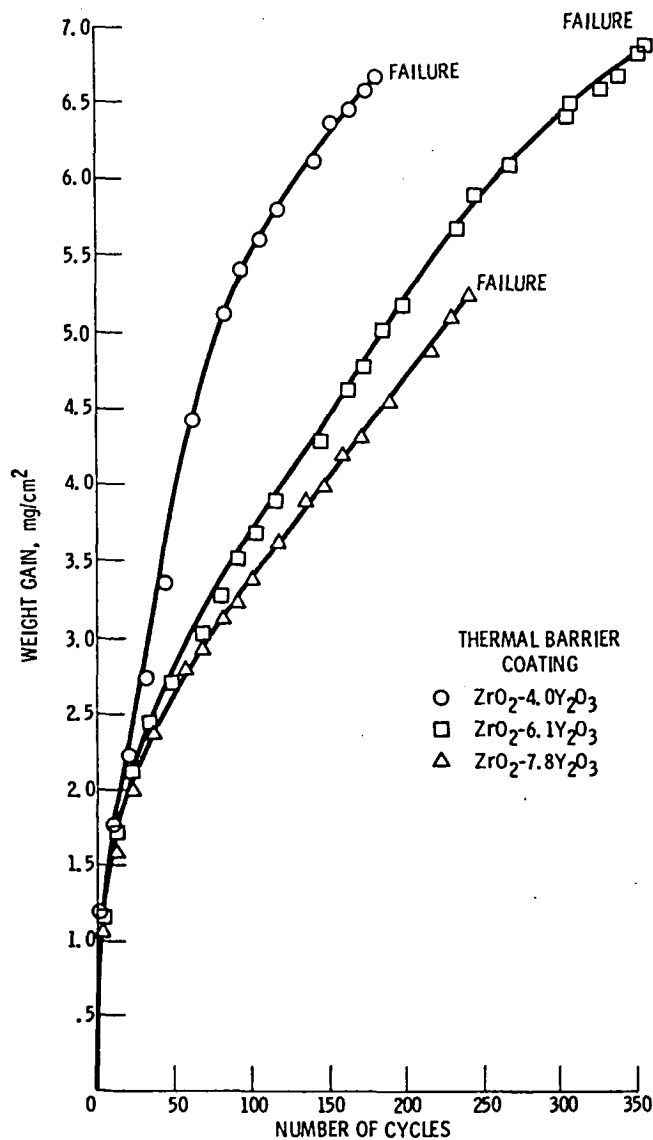
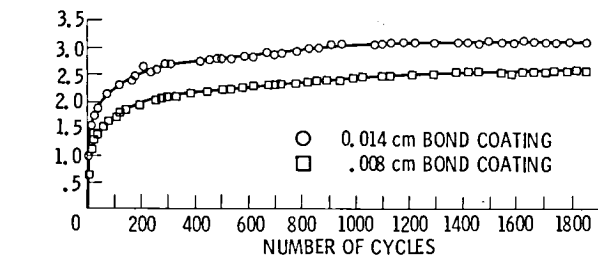
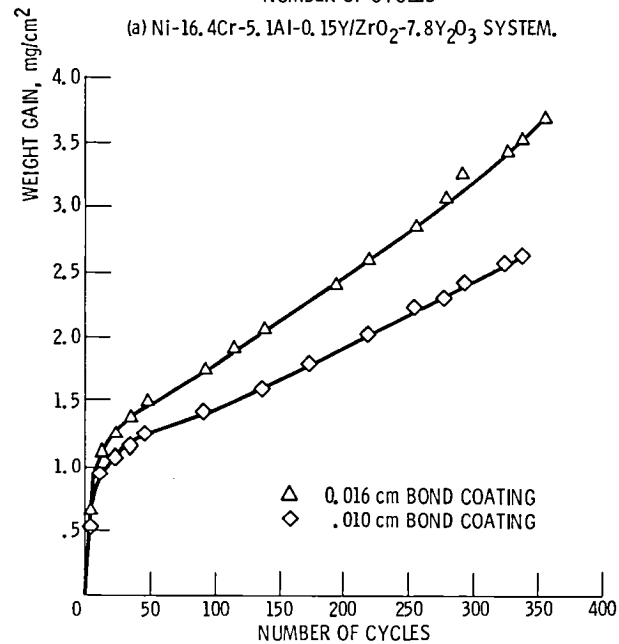


Figure 12. - Effect of yttria concentration in zirconia thermal barrier coating on specimen weight gain at 1095°C . (Cycle - 6-min heatup, 60 min at temperature, and 60 min of cooling to about 280°C .) Bond coating, Ni-16.4Cr-5.1Al-0.15Y.



(a) Ni-16.4Cr-5.1Al-0.15Y/ZrO₂-7.8Y₂O₃ SYSTEM.



(b) Ni-17.0Cr-5.4Al-0.35Y/ZrO₂-7.8Y₂O₃ SYSTEM.

Figure 13. - Effect of bond coating thickness on weight gain by thermal barrier system at 995° C. (Cycle - 6-min heatup, 60 min at temperature, and 60 min of cooling to about 280° C.)

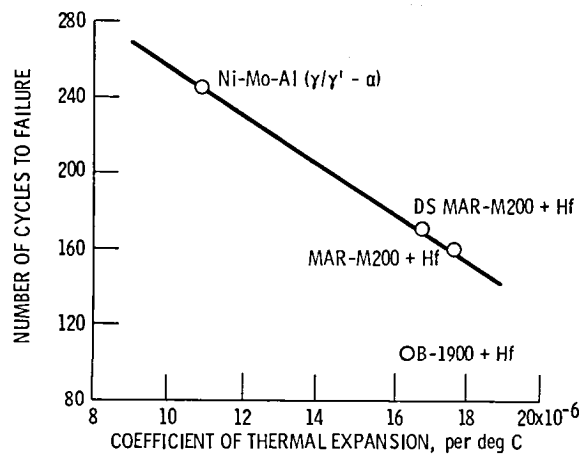


Figure 14. - Effect of coefficients of expansion of various substrate materials on life of Ni-16.4Cr-5.1Al-0.15Y/ZrO₂-7.8Y₂O₃ thermal barrier system as determined in cyclic furnace tests at 1095° C. (Cycle - 6-min heatup, 60 min at 1095°, and 60 min of cooling to about 280° C.)

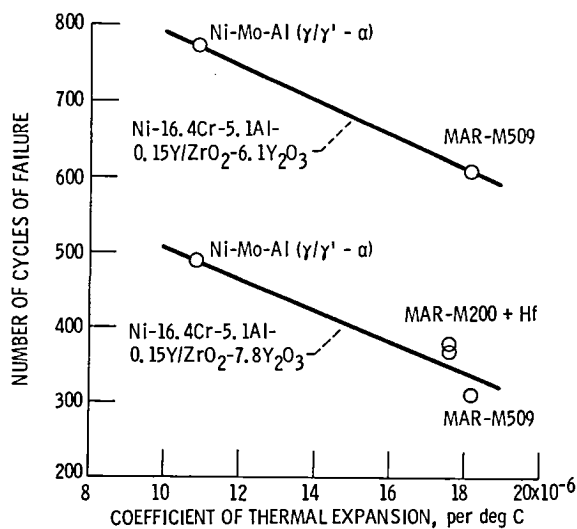


Figure 15. - Effect of coefficients of thermal expansion of various substrate materials on life of thermal barrier system as determined in a cyclic natural gas - oxygen torch rig at about 1250° C. (Cycle - 3-min heatup, 60 min at 1250° C, and 5 min of cooling to about 100° C.)

1. Report No. NASA TM-81604	2. Government Accession No.	3. Recipient's Catalog No.	
4. Title and Subtitle PERFORMANCE OF TWO-LAYER THERMAL BARRIER SYSTEMS ON DIRECTIONALLY SOLIDIFIED Ni-Al-Mo AND COMPARATIVE EFFECTS OF ALLOY THERMAL EXPANSION ON SYSTEM LIFE		5. Report Date October 1980	
		6. Performing Organization Code	
7. Author(s) Stephan Stecura		8. Performing Organization Report No. E-453	
		10. Work Unit No.	
9. Performing Organization Name and Address National Aeronautics and Space Administration Lewis Research Center Cleveland, Ohio 44135		11. Contract or Grant No.	
		13. Type of Report and Period Covered Technical Memorandum	
12. Sponsoring Agency Name and Address National Aeronautics and Space Administration Washington, D. C. 20546		14. Sponsoring Agency Code	
15. Supplementary Notes			
16. Abstract A promising two-layer thermal barrier coating system (TBS), Ni-16.4Cr-5.1Al-0.15Y/ZrO ₂ -6.1Y ₂ O ₃ (all in weight percent), was identified for directionally solidified Ni-Al-Mo ($\gamma/\gamma' - \alpha$). In cyclic furnace tests at 1095° C this system on $\gamma/\gamma' - \alpha$ was better than Ni-16.4Cr-5.1Al-0.15Y/ZrO ₂ -7.8Y ₂ O ₃ by about 50 percent. In natural gas - oxygen torch rig tests at 1250° C the ZrO ₂ -6.1Y ₂ O ₃ coating was better than the ZrO ₂ -7.8Y ₂ O ₃ coating by 95 percent on MAR-M509 substrates and by 60 percent on $\gamma/\gamma' - \alpha$ substrates. Decreasing the coefficient of thermal expansion of the substrate material from $17-18 \times 10^{-6}/^{\circ}\text{C}$ (MAR-M200 + Hf and MAR-M509) to $11 \times 10^{-6}/^{\circ}\text{C}$ ($\gamma/\gamma' - \alpha$) also resulted in improved TBS life. For example, in natural gas - oxygen torch rig tests at 1250° C, the life of Ni-16.4Cr-5.1Al-0.15Y/ZrO ₂ -6.1Y ₂ O ₃ was about 30 percent better on $\gamma/\gamma' - \alpha$ than on MAR-M509 substrates. Thus compositional changes in the bond and thermal barrier coatings were shown to have a greater effect on TBS life than does the coefficient of thermal expansion.			
17. Key Words (Suggested by Author(s)) Thermobarrier; Alloy; Oxide; Bond coating; Thermoexpansion		18. Distribution Statement Unclassified - unlimited STAR Category 26	
19. Security Classif. (of this report) Unclassified	20. Security Classif. (of this page) Unclassified	21. No. of Pages 34	22. Price* A03

National Aeronautics and
Space Administration

Washington, D.C.
20546

Official Business
Penalty for Private Use, \$300

SPECIAL FOURTH CLASS MAIL
BOOK

Postage and Fees Paid
National Aeronautics and
Space Administration
NASA-451



NASA

POSTMASTER: If Undeliverable (Section 158
Postal Manual) Do Not Return
